

REPORT DOCUMENTATION PAGE					Form Approved OMB No. 0704-0188	
<p>The public reporting burden for this collection of information is estimated to average 1 hour per response, including the time for reviewing instructions, searching existing data sources, gathering and maintaining the data needed, and completing and reviewing the collection of information. Send comments regarding this burden estimate or any other aspect of this collection of information, including suggestions for reducing the burden, to Department of Defense, Washington Headquarters Services, Directorate for Information Operations and Reports (0704-0188), 1215 Jefferson Davis Highway, Suite 1204, Arlington, VA 22202-4302. Respondents should be aware that notwithstanding any other provision of law, no person shall be subject to any penalty for failing to comply with a collection of information if it does not display a currently valid OMB control number.</p> <p>PLEASE DO NOT RETURN YOUR FORM TO THE ABOVE ADDRESS.</p>						
1. REPORT DATE (DD-MM-YYYY) 01-09-2006		2. REPORT TYPE REPRINT			3. DATES COVERED (From - To)	
4. TITLE AND SUBTITLE High-level Spacecraft charging in eclipse at geosynchronous altitudes: a statistical study				5a. CONTRACT NUMBER		
				5b. GRANT NUMBER		
				5c. PROGRAM ELEMENT NUMBER 61102F		
				5d. PROJECT NUMBER 5021		
6. AUTHOR(S) Shu T. Lai Maurice Tautz*				5e. TASK NUMBER RS		
				5f. WORK UNIT NUMBER A1		
7. PERFORMING ORGANIZATION NAME(S) AND ADDRESS(ES) Air Force Research Laboratory/VSBXT 29 Randolph Road Hanscom AFB, MA 01731-2010				8. PERFORMING ORGANIZATION REPORT NUMBER AFRL-VS-HA-TR-2006-1089		
9. SPONSORING/MONITORING AGENCY NAME(S) AND ADDRESS(ES)				10. SPONSOR/MONITOR'S ACRONYM(S) AFRL/VSBXT		
				11. SPONSOR/MONITOR'S REPORT NUMBER(S)		
12. DISTRIBUTION/AVAILABILITY STATEMENT Approved for public release; distribution unlimited						
13. SUPPLEMENTARY NOTES Approved for public release; distribution unlimited. REPRINTED FROM: J. Geophysical Research, Vol. 111, A09201. doi:10.1029/2004JA010733. Copyright 2006 by the American Geophysical Union. *AER/Radex, Inc., Lexington, MA						
14. ABSTRACT We present the results of a statistical study on high-level (above -200V in magnitude) negative-voltage spacecraft charging in eclipse at geosynchronous altitudes. Theoretically, there exists a critical temperature T^* for a surface material. Below T^* , no spacecraft charging occurs. Since T^* depends on the surface material, which differs from satellite to satellite, each is expected to have its own critical temperature. The theoretical results are compared with the coordinated space-environmental parameter data obtained by the Los Alamos National Laboratory (LANL) geosynchronous satellites. The LANL data include spacecraft charging events measured on several geosynchronous satellites, in eclipse and in sunlight, over several years. We have found a nearly linear trend, or better described by a quadratic one, between the spacecraft potential and the ambient electron temperature for potentials below in magnitude of about -5 kV. Extrapolation of the linear trend to zero volts shows an intercept at a finite temperature which agrees reasonably well with the critical temperature predicted by theory. The existence of a critical electron temperature is useful for informing decision and operational support of geosynchronous spacecraft with enhanced knowledge						
15. SUBJECT TERMS Critical temperature Spacecraft charging Plasma temperature						
16. SECURITY CLASSIFICATION OF:			17. LIMITATION OF ABSTRACT		18. NUMBER OF PAGES	
a. REPORT UNCL	b. ABSTRACT UNCL	c. THIS PAGE UNCL	UNL		19a. NAME OF RESPONSIBLE PERSON Shu T. Lai	
					19b. TELEPHONE NUMBER (Include area code)	



High-level spacecraft charging in eclipse at geosynchronous altitudes: A statistical study

Shu T. Lai¹ and Maurice Tautz²

Received 10 August 2004; revised 21 April 2006; accepted 16 May 2006; published 1 September 2006.

[1] We present the results of a statistical study on high-level (above -200V in magnitude) negative-voltage spacecraft charging in eclipse at geosynchronous altitudes. Theoretically, there exists a critical temperature T^* for a surface material. Below T^* , no spacecraft charging occurs. Since T^* depends on the surface material, which differs from satellite to satellite, each is expected to have its own critical temperature. The theoretical results are compared with the coordinated space-environmental parameter data obtained by the Los Alamos National Laboratory (LANL) geosynchronous satellites. The LANL data include spacecraft charging events measured on several geosynchronous satellites, in eclipse and in sunlight, over several years. We have found a nearly linear trend, or better described by a quadratic one, between the spacecraft potential and the ambient electron temperature for potentials below in magnitude of about -5 kV . Extrapolation of the linear trend to zero volts shows an intercept at a finite temperature which agrees reasonably well with the critical temperature predicted by theory. The existence of a critical electron temperature is useful for informing decision and operational support of geosynchronous spacecraft with enhanced knowledge.

Citation: Lai, S. T., and M. Tautz (2006), High-level spacecraft charging in eclipse at geosynchronous altitudes: A statistical study, *J. Geophys. Res.*, 111, A09201, doi:10.1029/2004JA010733.

1. Introduction

[2] Spacecraft charging can detrimentally affect electrical operations on space systems. Many communication and surveillance spacecraft are at geosynchronous altitudes and many more such spacecraft will be deployed in this new millennium. The plasma density in the geosynchronous environment varies from 0.1 cm^{-3} to more than 100 cm^{-3} , and the energy varies from a few eV to tens of keV, depending on local time and geomagnetic conditions. Spacecraft surface charging occurs in the presence of ambient plasma fluxes of high energies (keVs). While surface material properties and spacecraft geometry are defined by spacecraft design, spacecraft charging is controlled by the plasma conditions, which vary in time. If all the parameters characterizing the space plasma environment were known at every point in space and time, one could calculate the potential of every spacecraft as accurately as the available theoretical or computational model allows. In practice, very few spacecraft are well equipped to measure the space plasma parameters. It is, therefore, useful to identify the most important space-environment parameters for predicting spacecraft charging by using some space-environment forecast models.

[3] It has been postulated that the most reliable space-environment parameter for predicting spacecraft charging is plasma electron temperature. Historically, Rubin *et al.* [1980], first reported, though with only a few data points, the linear dependence of spacecraft potential as a function of ambient electron temperature. Their graph of spacecraft potential versus electron temperature showed an intercept at a finite temperature. Lai *et al.* [1982, 1983] and Laframboise *et al.* [1982] proposed that this finite minimum temperature was physical. Below this critical temperature, spacecraft charging does not occur; above it, charging does occur. Although this theory is now included in one of the standard textbooks on spacecraft-plasma interactions [Hastings and Garrett, 1996], it would be better accepted if there were substantial evidence obtained on multiple spacecraft. Lai and Della-Rose [2001] found evidence to support the theory by using one month of data obtained by the single Los Alamos National Laboratory (LANL) satellite LANL-94-084. The closest study that appears in print is in the documentation of Thomsen *et al.* [1999].

[4] This paper expands the Lai and Della-Rose [2001] study to include four more satellites (five total) and several years of data. The confidence in the critical temperature can be raised to a new level if it is based on a much larger database. We have examined the values of potential and electron temperature derived from flux measurements taken by LANL instruments. The data are filtered to only include points with potential values between 200 and 6000 volts negative. The relation between the potential and temperature can be fitted by a straight line, or somewhat better by a quadratic, with (in both cases) a positive value of the

¹Space Vehicles Directorate, Air Force Research Laboratory, Hanscom Air Force Base, Massachusetts, USA.

²AER/Radex Inc., Lexington, Massachusetts, USA.

20060926079

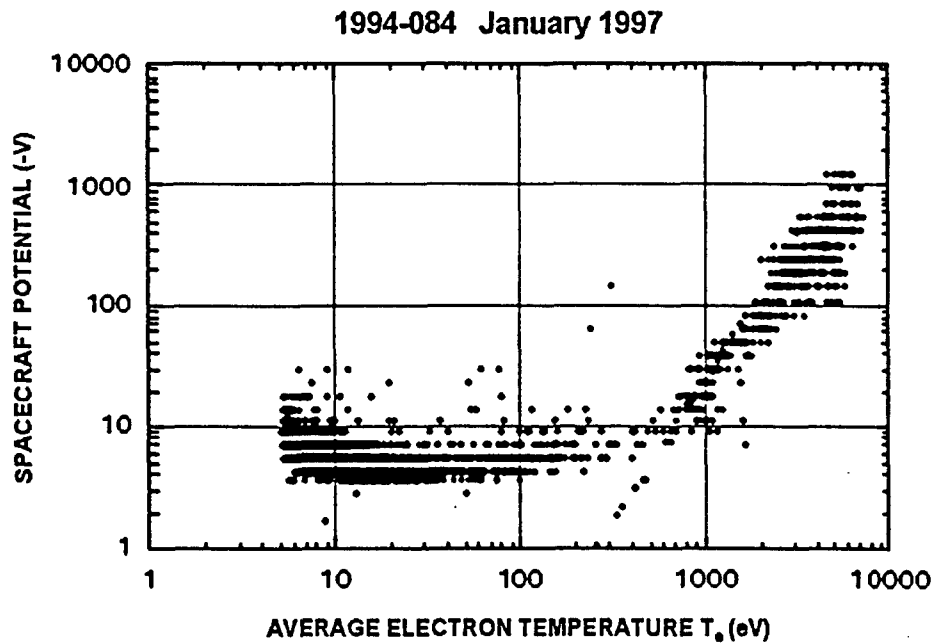


Figure 1. Empirical relationship between the measured spacecraft potential and the average electron temperature of the ambient plasma. [Thomsen *et al.*, 1999].

temperature at zero potential. For cleanliness of data analysis and presentation, we have omitted the potential points below a cutoff value $\phi_C = 200$ V. In retrospect, it would be sufficient to set ϕ_C as low as 60 V. At low voltages (below ϕ_C), charging can occur at very low electron temperature values. In plotting the charging level vs. the electron temperature (Figure 1), these low-level potential points (well below ϕ_C and are around 10V mostly) do not follow the straight line (or nearly straight line) which most of the points above ϕ_C follow. These low-level voltage points appear to be random. Since low-level charging is usually unavoidable but harmless to instruments, we will not attempt to study the cause of this low voltage complication. For the present study, we omit the points below ϕ_C . Thus the term “critical temperature” in the rest of the paper will refer only to temperature determined for values greater than ϕ_C and less than 6 kV.

[5] The new satellites include the Los Alamos National Laboratory (LANL) geosynchronous satellites LANL-89-046, LANL-90-95, LANL-91-80, LANL-94-084 and LANL-97A. The evidence for the existence of a critical temperature was seen for all LANL satellites studied.

2. Physics of Spacecraft Charging Onset

[6] At a given electron temperature, plasma electrons are faster than plasma ions by two orders of magnitude, because electrons are much lighter, and therefore faster, than ions. As a result, an object placed in plasma intercepts greater electron flux than ion flux. Indeed, measurements on the SCATHA satellite and the LANL-94-084 satellites showed that the electron flux was nearly two orders of magnitude higher than the flux of ions [Reagan *et al.*, 1983; Lai and Della-Rose, 2001]. Since the ambient ion current is so much smaller, it can normally be neglected in the threshold

calculations, although there are exceptional events that we do not consider here.

[7] Since the incoming flux of electrons exceeds that of positive ions, a spacecraft becomes negatively charged to a potential for which the repulsion of ambient electrons and attraction of ions cause the surface currents to balance. We are not interested here in low voltage charging (a few tens of volts negative) because it usually does no harm to electronic instruments on spacecraft. At higher energies, secondary and backscattered electrons (both outgoing) become important [Sternglass, 1954a, 1954b]. For most surface materials, the secondary electron coefficient $\delta(E)$ (Figure 2, bottom), defined as the number of secondary electrons generated for every primary electron, starts at zero primary electron energy and exceeds unity at the first crossing point E_1 (60 eV typically, depending on the material) until the second crossing point E_2 (1500 eV typically, depending on the material). The backscattered electron coefficient $\eta(E)$, defined as the number of incoming electrons scattered by the surface material to space, is small typically, depending on the material [Prokopenko and Laframboise, 1980]. Therefore primary electrons in the range E_1 to E_2 tend to charge the spacecraft surfaces to positive voltages, while primary electrons of energies greater than E_2 tend to charge the surfaces to negative voltages. As a result, primary electrons in an energy distribution can be thought of as being in two parts, one responsible for positive charging and the other for negative charging. Which part wins depends on their competition of outgoing and incoming fluxes.

[8] Consider a Maxwellian electron distribution $f(E)$ of temperature T . At low temperature, the low-energy electrons are enhanced so the low-energy part is likely to win. As the temperature increases, there are more and more electrons in the high-energy part (Figure 2, top). There should be a temperature (critical temperature T^*) above which the high-energy part wins and therefore charging to negative poten-

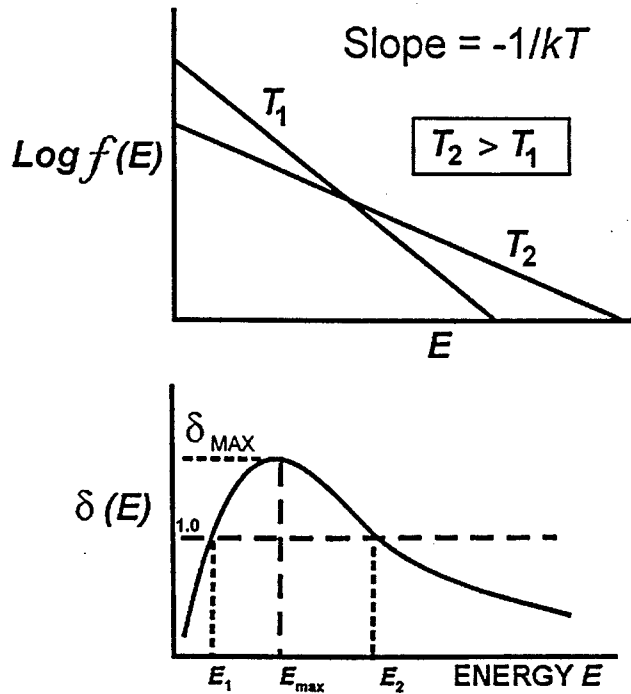


Figure 2. (top) Log function of primary electron distributions with different temperatures. The one with higher temperature has more electrons at higher energies. (bottom) Secondary electron emission coefficient $\delta(E)$ as a function of primary electron energy E . The primary electrons of high energies beyond the second crossing of unity ($\delta(E) = 1$) are responsible for negative-voltage charging while the primary electrons between the two crossings are responsible for positive-voltage charging.

tials occur. A mathematical formulation of this idea is as follows.

[9] We do not consider the ion currents. Assume that the ambient electron temperature is low but increasing and the satellite is initially uncharged. At the threshold of charging, the currents of the incoming ambient electrons and the outgoing secondary and backscattered electrons balance with each other as follows.

$$\int_0^{\infty} dE E f(E) = \int_0^{\infty} dE E [\delta(E) + \eta(E)] f(E) \quad (1)$$

where $\delta(E)$ and $\eta(E)$ are the coefficients of secondary electron emission and backscattered electron emission respectively. For a Maxwellian space plasma, the distribution function $f(E)$ is of the form:

$$f(E) = n(m/2\pi kT)^{3/2} \exp(-E/kT) \quad (2)$$

Substituting equation (2) into equation (1), one readily obtains two results: (1) Since the density n is multiplicative, it can be canceled on both sides, so the threshold condition is independent of plasma density n . (2) The variable T can be solved for in equations (1) and (2), and it is defined as T^* , the critical temperature for the onset of negative voltage spacecraft charging. To calculate the actual values of T^* in

equations (1) and (2), one needs to put in the functions $\delta(E)$ and $\eta(E)$. If the primary electrons are coming in at various angles, θ , one needs to use the angle-dependent functions of $\delta(E, \theta)$ and $\eta(E, \theta)$. The algebra becomes more complicated when the incident angles are included. For typical materials, T^* is found to be a few keV [Lai et al., 1982, 1983; Laframboise et al., 1982; Laframboise and Kamitsuma, 1983; Lai and Della-Rose, 2001].

3. Spacecraft Potential

[10] For the onset of spacecraft charging, we have neglected the ions because their flux is about two orders of magnitude smaller than that of the ambient electrons. Once negative-voltage charging occurs, the ambient positive ions are attracted toward the spacecraft. Therefore, to determine the resulting spacecraft equilibrium (negative) potential, one needs to include the ions in the consideration of current balance.

[11] For a given ambient current, the time needed to charge a surface to a given potential depends on the capacitance [Hastings and Garrett, 1996]. For a simple uniform surface, the time is of the order of milliseconds for a spacecraft with a radius on the order of meters. For surfaces of large capacitance, such as those having thin dielectric layers, it takes much longer to charge. In either case, when the surface currents are unbalanced the potential moves, typically to negative values, repelling electrons and attracting ions, until balance is restored.

[12] Secondary electrons resulting from primary-electron impact on surfaces play an important role in spacecraft charging, while secondary electrons from ion impact, which require much higher primary energy, are not important until the primary energy exceeds several keV and thus are not significant at low energies. Lai and Della-Rose [2001] showed that any effect of ion-impact-induced secondary electrons on spacecraft potential can be ignored below about 3 kV in magnitude.

[13] For spacecraft-charging calculations, it is often a good approximation to use the Langmuir orbit-limited equation [Mott-Smith and Langmuir, 1926] to describe the current balance:

$$I_i(\phi) - I_e(\phi) = \mu I_i(0) \left[1 - \frac{q_i \phi}{kT_i} \right]^\alpha - I_e'(0) \exp\left(-\frac{q_e \phi}{kT_e}\right) = 0 \quad (3)$$

where

$$I_e'(\phi) = I_e(0)[1 - (\delta + \eta)]$$

and δ and η are the secondary and backscatter electron emissions respectively. In equation (3), $I_e(\phi)$ and $I_i(\phi)$ are the electron and ion currents, respectively, collected by the spacecraft at potential ϕ (< 0) relative to the space plasma. In this equation, $q_i = e$, $q_e = -e$, where e is the elementary charge ($e > 0$). If the spacecraft is cylindrical, μ equals approximately $2/\pi^{1/2}$ (≈ 1.1) and the square bracket in the ion-attraction term (equation (3)) should be raised to a power of $\alpha = 1/2$ [Langmuir, 1960]. If the spacecraft is spherical, μ equals approximately 1.0 and $\alpha = 1$. The attraction term is only valid in the Langmuir orbit-limited

regime [Langmuir, 1960]. The conditions for this regime are approximately met in the geosynchronous environment. The derivation of the attraction term [Mott-Smith and Langmuir, 1926] does not require the assumptions of $q\phi < kT$. The derivation of the current collection terms can be based on a uniform, isotropic ambient Maxwellian plasma distribution and orbit-limited conditions.

[14] The normalized current of the (outgoing) secondary and backscattered electrons is given by [Lai, 1991; Lai and Della-Rose, 2001]:

$$\langle \delta + \eta \rangle = \frac{\int_0^\infty dE E f(E) [\delta(E) + \eta(E)]}{\int_0^\infty dE E f(E)} \quad (4)$$

If the ion current $I_i(0)$ is neglected in equation (3), one recovers the current balance condition at the charging threshold and the condition

$$\langle \delta + \eta \rangle = 1 \quad (5)$$

is identical to that given by equation (1). Since η is much less than 1 for most surface materials, some authors in the literature choose to approximate the condition (equation (5)) further by writing $\langle \delta \rangle = 1$; this is the form given by Hastings and Garrett [1996].

[15] One can reduce equation (3) to an approximately linear form by expanding in a Taylor series and keeping only the lowest-order term. We treat the ratio T_i/T_e as a constant although there is some measured variations as a function of ϕ [see Lai and Della-Rose, 2001, Figure 3]. For a spacecraft potential lower than the ambient ion temperature, that is, $e\phi \ll kT_i$, which is initially valid, one expands equation (3) in powers of $e\phi/kT_i$ and obtains

$$e\phi = kT_e \left(\frac{T_i/T_e}{T_i/T_e + \alpha} \right) \log \left(\frac{\mu I_i(0)}{I_e'(0)} \right) \quad (6)$$

which gives $e\phi$ approximately a straight line as a function of kT_e . For higher values of $e\phi$, the quadratic term needs to be included. Equation (6) is not really a straight line because the ratio T_i/T_e is not strictly constant and the log term is a function of T_e . In this form, the threshold value of T_e corresponds to $\log(1)$, which leads to

$$\langle \delta + \eta \rangle = 1 - \frac{\mu I_i(0)}{I_e'(0)} \approx 1 \quad (7)$$

which agrees with equation (5) when $I_i(0)$ is much smaller than $I_e(0)$.

4. Instrumentation and Calculation of Moments

[16] The magnetospheric plasma analyzers (MPA) fielded on several LANL geosynchronous satellites have been documented by Bame et al. [1993] and McComas et al. [1993]. The MPA instrument is a spherical-sector electrostatic analyzer for measuring three-dimensional energy-per-charge distributions of ions and electrons. In one satellite spin, the MPA views about 92% of the unit sphere, divided into six polar by 24 azimuthal view directions. As the satellite spins through each 15° azimuth sector, the

MPA voltage sweeps through 40 logarithmically spaced energy channels ranging from 40 keV/e down to 1 eV/e. The satellite spin period is about 10 s. The MPA data are processed to provide the spin-averaged fluxes at each of the 40 energy channels, and the moments of the particle distributions are also calculated. For details, we must refer the reader to the documents of Bame et al. [1993] and McComas et al. [1993].

[17] Thomsen et al. [1999] has documented the calculation of moments from measurements by the Los Alamos magnetospheric plasma analyzer (MPA). The moment equations of the density n , the vector velocity \mathbf{V} , and the three-dimensional temperature matrix \mathbf{T} are given as follows [Thomsen et al., 1999]:

$$n = \int f(\mathbf{v}) d^3\mathbf{v} \quad (8)$$

$$\mathbf{V} = (1/n) \int \mathbf{v} f(\mathbf{v}) d^3\mathbf{v} \quad (9)$$

$$\mathbf{T} = (1/n) \int m(\mathbf{v} - \mathbf{V})(\mathbf{v} - \mathbf{V}) f(\mathbf{v}) d^3\mathbf{v} \quad (10)$$

where the ions are assumed to be protons. The moments are computed only for records containing both complete three-dimensional ion and electron spectra. Further details on filtering for incomplete and bad data, decompression, dead-time correction, replacement of counts from bad detectors, background subtraction, etc. are given by Thomsen et al. [1999].

[18] When a spacecraft charges to a negative potential, ambient ions are attracted toward the spacecraft. The energy gained by an ion equals that of the spacecraft potential. As a result, a peak appears in the ion spectrum. The energy at which the peak is located corresponds to the spacecraft potential. The LANL algorithm searches the spin-averaged ion spectrum below 9 keV for the peak. To be a valid peak, the jump in ion count must be at least a factor of 2. This procedure leads to quantized charging levels, depending on the ion binning in the MPA instrument. Sometimes, when the ambient plasma density is unusually low, it is not possible to detect a clear ion peak. If neither a clear peak nor a clear zero-potential is found, the LANL algorithm uses an iterative procedure to estimate the spacecraft potential. Data obtained in this manner are so flagged. The procedure is based on the empirical relationship between the spacecraft potential ϕ and the average electron temperature T_a defined as follows:

$$T_a = [(n_{lp} \times 5.0 \text{ eV}) + (n_{he} \times T_{he})] / (n_{lp} + n_{he}) \quad (11)$$

where the subscripts lp and he denote low-energy protons and high-energy electrons. The low-energy proton density is a proxy for the electrons and the low-energy electron temperature is approximated as 5.0 eV. The empirical relationship adopted is of the form:

$$\phi = -A - B \times (T_a/T_o)^D \quad (12)$$

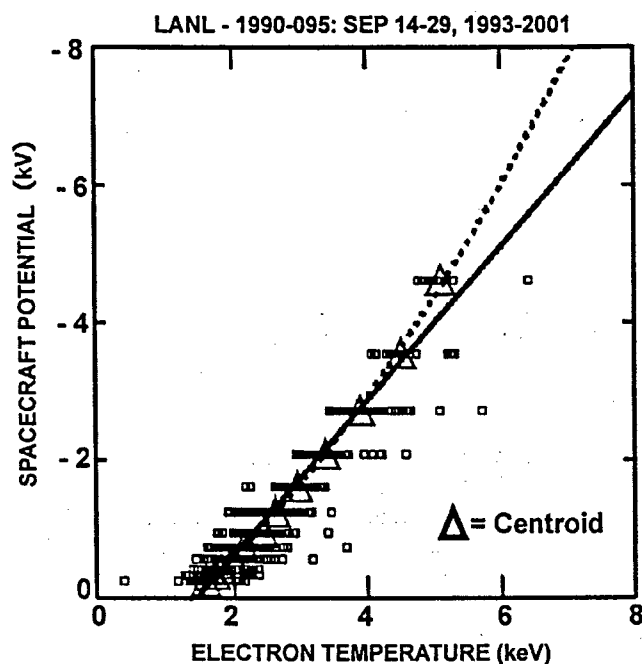


Figure 3. Spacecraft potential and electron temperature measured on Spacecraft LANL-1990-095, during eclipse periods, 14–29 September 1993–2001.

where the parameters A , B , T_0 and D are determined for each satellite. For further details, see *Thomsen et al.* [1999].

[19] We have examined the flagged data points in three different months of sample data (courtesy M. F. Thomsen, 2002) and found that the flagged data are all on the sunlight charging curve and none on the eclipse charging curve. There are other types of flags corresponding to various uncertainties, but they are so rare that the total number of them amounts to less than 1% of all data. Therefore we conclude that the flagged data of interpolation do not affect our eclipse-charging study at all and the other types of flagged data amount to a small percent of the fluctuations.

[20] There are two different definitions of temperatures used in this paper. Temperature T is in the definition of Maxwellian distribution in equation (2) and the measured temperature T_M occurs in kinetic definition (equation (10)). If the ambient electron distribution is Maxwellian, one can show by using mathematical techniques, commonly used in statistical physics, that the two temperatures are equivalent and, furthermore, the temperatures are invariant under any surface charging level ϕ . However, if the distribution deviates from being Maxwellian, there is no guarantee that the temperature so measured is not affected by the charging level. The Maxwellian distribution allows one to obtain results as a guide, whereas for an arbitrary distribution, there is no way to conduct any meaningful analytical treatment. It is assumed that the Maxwellian results serve as an average of arbitrary distributions deviating on both sides of the Maxwellian. Indeed, as shown in the next section, there are deviations on both sides from the Maxwellian trend at the low charging voltages that were considered. However, we make the basic caveat that the measured temperature is

generally not the same as the temperature of a Maxwellian fit, either theoretically or in practice.

5. Observation of Spacecraft Charging in Eclipse

[21] In choosing the eclipse data for analysis, we limited our data to those obtained during the 15 days period centered on the equinoxes and to midnight local time plus or minus half an hour. The data were collected over the lifetime of each satellite. We have obtained ten graphs, corresponding to the two equinoxes and the five satellites. We have chosen only the range of potentials: -6000 to -200 volts. The -200 volt limit was made as discussed in section 1. The -6000 volts limit was made because measurements above that level are unreliable (M. F. Thomsen, personal communication, 1999).

[22] Because the graphs are similar to each other, we need only show three of the ten graphs. These are given in Figures 3–5 for three different satellite and two different equinoxes. The figures show spacecraft potential vs. electron temperature. Each of the results shows (1) the trend of each plot is almost a straight line, (2) there exists an intercept T^* (its value being approximately 1 to 2 keV), and (3) a quadratic function would fit better than a straight line. The spread in temperature at each voltage level is partially due to the quantized voltage level spacing.

[23] To aid in the analysis, centroids (large triangles in Figures 3–5) were calculated at each (quantized) voltage level, and the fits were made to them. A centroid is the average temperature of all the points on the same voltage level. Both linear and quadratic fits were made using the IDL least squares weighted polynomial fitting routine POLYFITW. The linear fits were done first to establish the ($y = 0$) intercept, which is the critical temperature T^* .

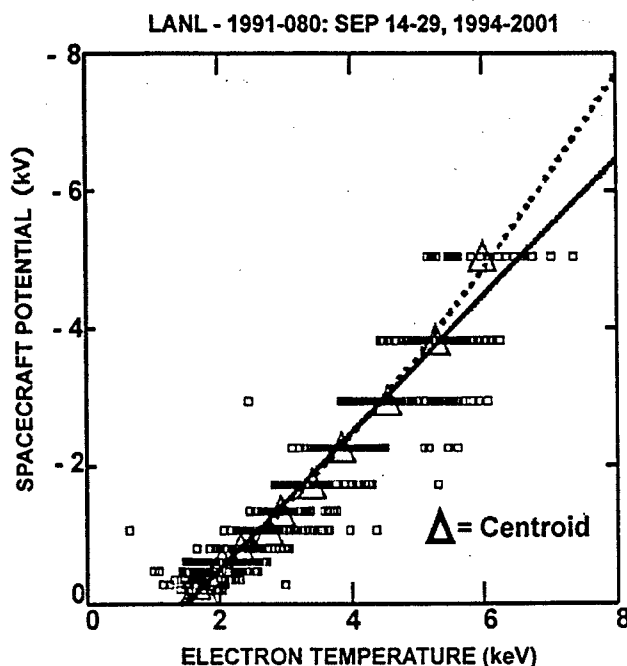


Figure 4. Spacecraft potential and electron temperature measured on Spacecraft LANL-1991-080, during eclipse periods, 14–29 September 1994–2001.

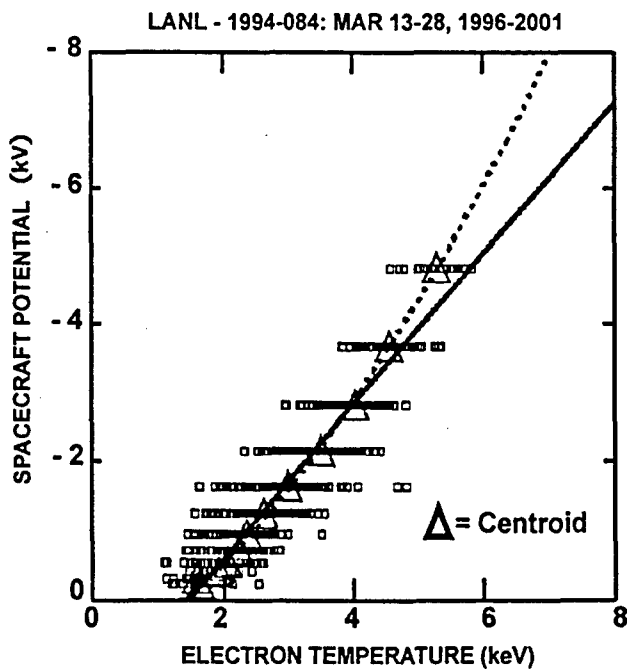


Figure 5. Spacecraft potential and electron temperature measured on Spacecraft LANL-1994-084, during eclipse periods, 13–28 March 1996–2001.

The quadratic fits were done next. The quadratic fits were found to be unstable in that an intercept did not always occur. To help stabilize the quadratic fits an extra data point was added which represented the intercept taken from the linear fits.

[24] The straight line fit of each plot suggests that the observed spacecraft potential ϕ is approximately proportional to the electron temperature kT_e . This observed behavior agrees with that predicted by equation (3), even though the theoretical model is admittedly simple. The deviation from a straight line can be due to several possible reasons. (1) One needs to include the quadratic term as ϕ/kT_e increases. (2) The ambient electron distribution may deviate from Maxwellian and resembles a kappa distribution [Meyer-Vernet, 1999] at high temperatures, when fresh and significant plasma disturbances arrive, possibly from the Sun or the magnetotail. (3) The ratio T_i to T_e is only an approximate constant as can be seen in Figure 3 of Lai and Della-Rose [2001]. These three reasons are not mutually exclusive and can compete with each other. That the relation

between the spacecraft potential and temperature is linear, as it would be for a Maxwellian plasma is what is surprising, not that relationship becomes quadratic at higher temperatures. This is because measured geosynchronous spectra are complex and not at equilibrium during charging events so that a Maxwellian fit is typically very poor.

[25] The intercept T^* is found to be from 0.9 to 1.6 keV in this study. These values are in the range of critical temperatures computed using the secondary electron coefficients [Sanders and Inouye, 1978] and backscattered electron coefficients [Prokopenko and Laframboise, 1980] for typical spacecraft surface materials. A better comparison is not possible because the surface materials of the subject satellites are unknown. If each satellite has a different main surface material, each satellite would have a different critical temperature. Table 1 summarizes the standard deviation, sigma, for the fits and the value found for T^* , along with statistical errors. Table 1 shows that a quadratic fit is significantly better and that the error bars are large. The T^* are lower with the quadratic fits, but are the same order of magnitude. The large values of sigma indicate that the temperature, as defined in this paper, alone is not adequate for high confidence predictions.

6. A Case Study for a Storm Event

[26] A major geomagnetic event in the recent solar maximum was the Bastille Day (14 July 2000) storm. Figure 6 shows the magnetic index K_p rising to the highest possible value ($K_p = 9$) during the storm. The parallel and perpendicular electron temperatures measured on the LANL 1994-084 Satellite rose to high values upon the arrival of the solar disturbance. The electron density rose later; the rise was not simultaneously with the electron temperature. This case offers a good opportunity to observe the response of the potential to these two space parameters, namely, electron temperature and electron density. Indeed, the data measured on LANL 1994-084 show that the spacecraft potential and the electron temperature rose and fell together but they showed no correlation with the electron density at all. This case indicates that the electron density was not the principal factor in spacecraft charging, as predicted by the critical temperature theory.

7. Summary and Discussion

[27] We have presented the theory and observation of critical temperature, which is the threshold temperature for

Table 1. Summary of IDL Least squares Polynomial Fits

LANL Satellite Name	Eclipse Month	Linear Fit Sigma, eV	Linear Fit Intercept, eV	Quadratic Fit Sigma, eV	Quadratic Fit Intercept, eV
1989-046	Mar	365.8	1073.3 \pm 95.6	199.6	885.7 \pm 149.1
1989-046	Sep	243.2	1281.1 \pm 72.8	110.3	1156.1 \pm 75.5
1990-095	Mar	423.7	1299.5 \pm 93.9	140.1	998.5 \pm 222.5
1990-095	Sep	185.9	1434.4 \pm 37.3	57.90	1367.3 \pm 29.9
1991-080	Mar	162.9	1609.7 \pm 27.5	138.0	1588.7 \pm 30.4
1991-080	Sep	194.5	1485.1 \pm 37.8	95.4	1424.9 \pm 40.3
1994-084	Mar	222.7	1449.3 \pm 50.0	77.3	1363.6 \pm 50.4
1994-084	Sep	232.2	1366.1 \pm 63.8	118.9	1263.7 \pm 65.0
1997A	Mar	240.0	1537.4 \pm 88.1	189.6	1443.7 \pm 130.3
1997A	Sep	186.4	1618.0 \pm 47.2	92.4	1551.1 \pm 50.6

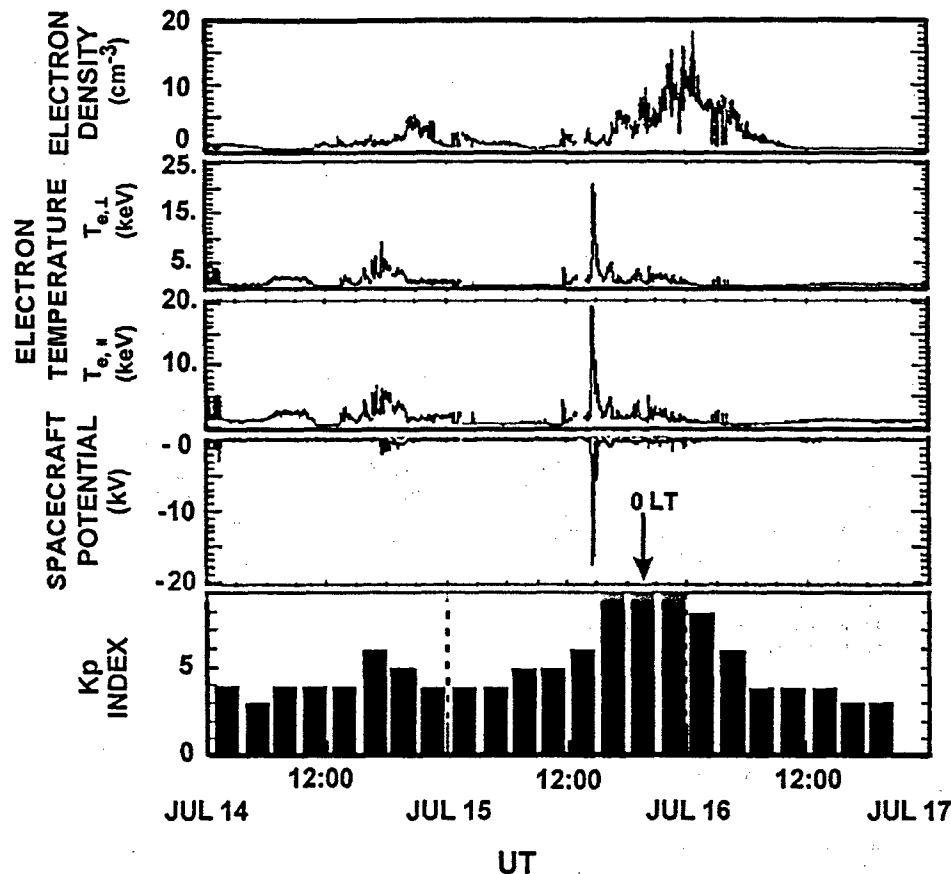


Figure 6. History of spacecraft potential, electron density, electron temperatures, and K_p index in the Bastille Day, 2000, geomagnetic storm.

high-voltage spacecraft charging to commence. The idea of critical temperature stems from the property of secondary electron emission which plays an important role in the charging of spacecraft surfaces. The critical temperature is relevant to charging to high negative voltages. In this paper, we study the data of high-level charging between $-200V$ and $-6000V$.

[28] To derive the critical temperature, one ignores the ambient ion flux because it is two orders of magnitude smaller than that of the ambient electrons. The current balance is between incoming ambient electrons and the sum of the outgoing secondary and backscattered electrons only. The generally computed critical temperatures for various materials values are between 1.0 to 2.5 keV [Lai and Della-Rose, 2001]. Once charging (to negative potentials) occurs, the ambient ions are attracted while the ambient electrons are repelled. Therefore, to determine the spacecraft potential, one needs to include the ambient ions as well in the theoretical formulation.

[29] In recent years, the coordinated data of spacecraft charging and other space environmental parameters measured on LANL satellites have become available. Using the data, we have found supporting evidence of the existence of critical temperature. Plotting the centroid of the spacecraft potential data versus electron temperature show almost straight lines. The lines are better described by quadratic curves. The results obtained by using different LANL satellite are consistent. The values of the critical temper-

atures are mostly between 1 to 2 keV depending on the surface materials, the spacecraft geometry, and the incoming angles of the ambient electrons which are unknown.

[30] There are deviations and fluctuations. The data fluctuations are partially due to the quantized voltage spacing. We have introduced centroids to reduce the effect of the fluctuations. The deviations become very noticeable at higher voltages from above 5 keV and a quadratic fit becomes better. There are reasons for deviating from a straight line at higher voltages. One reason is that the straight line approximation requires the ratio of voltage to temperature to be small but the ratio increases at higher voltages. Another reason is that the ambient electron distribution may not be Maxwellian when the space plasma is hot or disturbed but may resemble a kappa distribution. The latter resembles a Maxwellian but features an additional high-energy tail. The threshold charging problem with a kappa distribution is outside the scope of this paper.

[31] We contend that the theory of critical temperature provides an important method for indicating the onset of high-voltage spacecraft charging. Advantages of the method are that it uses only a single, well known variable, the electron temperature, and it is based on a clear physical effect, that of secondary emission. On the other hand, the calculation is indirect, requiring the second moment of the distribution function and the method assumes a Maxwellian distribution, which may be a poor approximation, leading to large error bars. That a statistical study of the potential as a

function of temperature gives a positive intercept with a computed value near those generally calculated for critical temperature provides additional support for the critical temperature theory. We hope that the results will be useful for serving the constellation of geosynchronous spacecraft by emphasizing that the electron temperature is an important parameter for decision making during spacecraft operations. We believe that system and space environment models which incorporate this will have improved prediction and forecast capabilities enabling spacecraft operators to make better decisions.

[32] **Acknowledgments.** The Los Alamos Magnetospheric Plasma Analyzer (MPA) measurements were obtained from the CDAWeb data service at NASA Goddard Space Flight Center. We thank M. Thomsen for permission to use the MPA data and for sending us the report [Thomsen et al., 1999] during the revision of our paper. Part of this work was supported by UPOS through Johns Hopkins University. The material of this paper has been presented at AGU where we benefited from the helpful comments and appreciation from the audience. We are grateful to Dave Knecht, Devin Della-Rose, and Shawn Young for reading the manuscript with helpful comments. The work of Maurice Tautz was done under contract F19628-00-C0089. The website of AER, Inc., is at <http://www.aer.com/>.

[33] Shadia Rifai Habbal thanks Victoria A. Davis and another referee for their assistance in evaluating this paper.

References

- Bame, S. J., D. J. McComas, M. F. Thomsen, B. L. Barraclough, R. C. Elphic, and J. P. Glore (1993), Magnetospheric plasma analyzer for spacecraft with constrained resources, *Rev. Sci. Instrum.*, **64**, 1026–1033.
- Hastings, D., and H. B. Garrett (1996), *Spacecraft-Environment Interactions*, Cambridge Univ. Press, New York.
- Laframboise, J. G., and M. Kamitsuma (1983), The threshold temperature effect in high voltage spacecraft charging, in *Proceedings of Air Force Geophysics Workshop on Natural Charging of Large Space Structures in Near Earth Polar Orbit*, AFRL-TR-83-0046, ADA-134-894, 293–308.
- Laframboise, J. G., R. Godard, and M. Kamitsuma (1982), Multiple floating potentials, threshold temperature effects, and barrier effects in high voltage charging of exposed surfaces on spacecraft, paper presented at International Symposium on Spacecraft Materials in Space Environment, Eur. Space Agency, Toulouse, France.
- Lai, S. T. (1991), Spacecraft charging thresholds in single and double Maxwellian space environments, *IEEE Trans. Nucl. Sci.*, **38**, 1629–1634.
- Lai, S. T., and D. Della-Rose (2001), Spacecraft charging at geosynchronous altitudes: New evidence of existence of critical temperature, *J. Spacecr. Rockets*, **38**, 922–928.
- Lai, S. T., M. S. Gussenhoven, and H. A. Cohen (1982), Energy range of ambient electrons responsible for spacecraft charging, *Eos Trans. AGU*, **63**(18), 421.
- Lai, S. T., M. S. Gussenhoven, and H. A. Cohen (1983), The concepts of critical temperature and energy cutoff of ambient electrons in high voltage charging of spacecraft, in *Proceedings of the 17th ESLAB Symposium*, edited by D. Guyenne and J. H. A. Pedersen, pp. 169–175, Eur. Space Agency, Noordwijk, Netherlands.
- Langmuir, I. (1960), *Collected Works of Irving Langmuir*, edited by C. G. Suits, Elsevier, New York.
- McComas, D. J., S. J. Bame, B. L. Barraclough, J. R. Donart, R. C. Elphic, J. T. Gosling, M. B. Moldwin, K. R. Moore, and M. F. Thomsen (1993), Magnetospheric plasma analyzer: Initial three-spacecraft observations from geosynchronous orbit, *J. Geophys. Res.*, **98**(A8), 13,453–13,466.
- Meyer-Vernet, N. (1999), How does the solar wind blow? A simple kinetic model, *Eur. J. Phys.*, **20**, 167–176.
- Mott-Smith, H. M., and I. Langmuir (1926), The theory of collectors in gaseous discharges, *Phys. Rev.*, **28**, 727–763.
- Prokopenko, S. M., and J. G. L. Laframboise (1980), High voltage differential charging of geostationary spacecraft, *J. Geophys. Res.*, **85**(A8), 4125–4131.
- Reagan, J. B., R. E. Meyerott, R. W. Nightingale, P. C. Filbert, and W. L. Imhoff (1983), Spacecraft charging currents and their effects on space systems, *IEEE Trans. Electr. Insulations*, **18**, 354–365.
- Rubin, A., H. B. Garrett, and A. H. Wendel (1980), Spacecraft charging on ATS-5, AFGL-TR-80-0168, ADA-090-508, Air Force Geophys. Lab., Hanscom Air Force Base, Mass.
- Sanders, N. L., and G. T. Inouye (1978), Secondary emission effects on spacecraft charging: energy distribution consideration, in *Spacecraft Charging Technology 1978*, edited by R. C. Finke and C. P. Pike, pp. 747–755, Air Force Geophys. Lab., Hanscom Air Force Base, Mass.
- Sternglass, E. J. (1954a), Theory of secondary electron emission, *Sci. Pap.* 1772, Westinghouse Res. Lab., Pittsburgh, Pa.
- Sternglass, E. J. (1954b), Backscattering of kilovolt electrons from solids, *Phys. Rev.*, **95**, 345–358.
- Thomsen, M. F., E. Noveroske, J. E. Borovsky, and D. J. McComas (1999), Calculation of moments from measurements by the Los Alamos magnetospheric plasma analyzer, *LANL Rep. LA-13566-MS*, Los Alamos Natl. Lab., Los Alamos, N. M.
- S. T. Lai, Space Vehicles Directorate, Air Force Research Laboratory, Hanscom Air Force Base, MA 01731-3010, USA. (shu.lai@hanscom.af.mil)
- M. Tautz, AER/Radex Inc., Lexington, MA 02421, USA.